Sea ice variations and trends during the Common Era in the Atlantic sector of the Arctic Ocean

Ana Lúcia Lindroth Dauner[1], Frederik Schenk[2,3,4], Katherine Elizabeth Power[3,5], Maija P. Heikkilä[1,6]

[1]Environmental Change Research Unit (ECRU), Ecosystems and Environment Research Programme, Faculty of Biological and Environmental Sciences, University of Helsinki, Helsinki, 00014, Finland
[2]Department of Geosciences and Geography, University of Helsinki, Helsinki, 00014, Finland
[3]Bolin Centre for Climate Research, Stockholm University, Stockholm, 10691, Sweden
[4]Department of Geological Sciences, Stockholm University, Stockholm, 10691, Sweden
[5]Department of Physical Geography, Stockholm University, Stockholm, 10691, Sweden
[6]Helsinki Institute of Sustainability Science (HELSUS), University of Helsinki, Helsinki, 00014, Finland

Correspondence to: Ana Lúcia Lindroth Dauner (ana.lindrothdauner@helsinki.fi; anadauner@gmail.com)

Figures

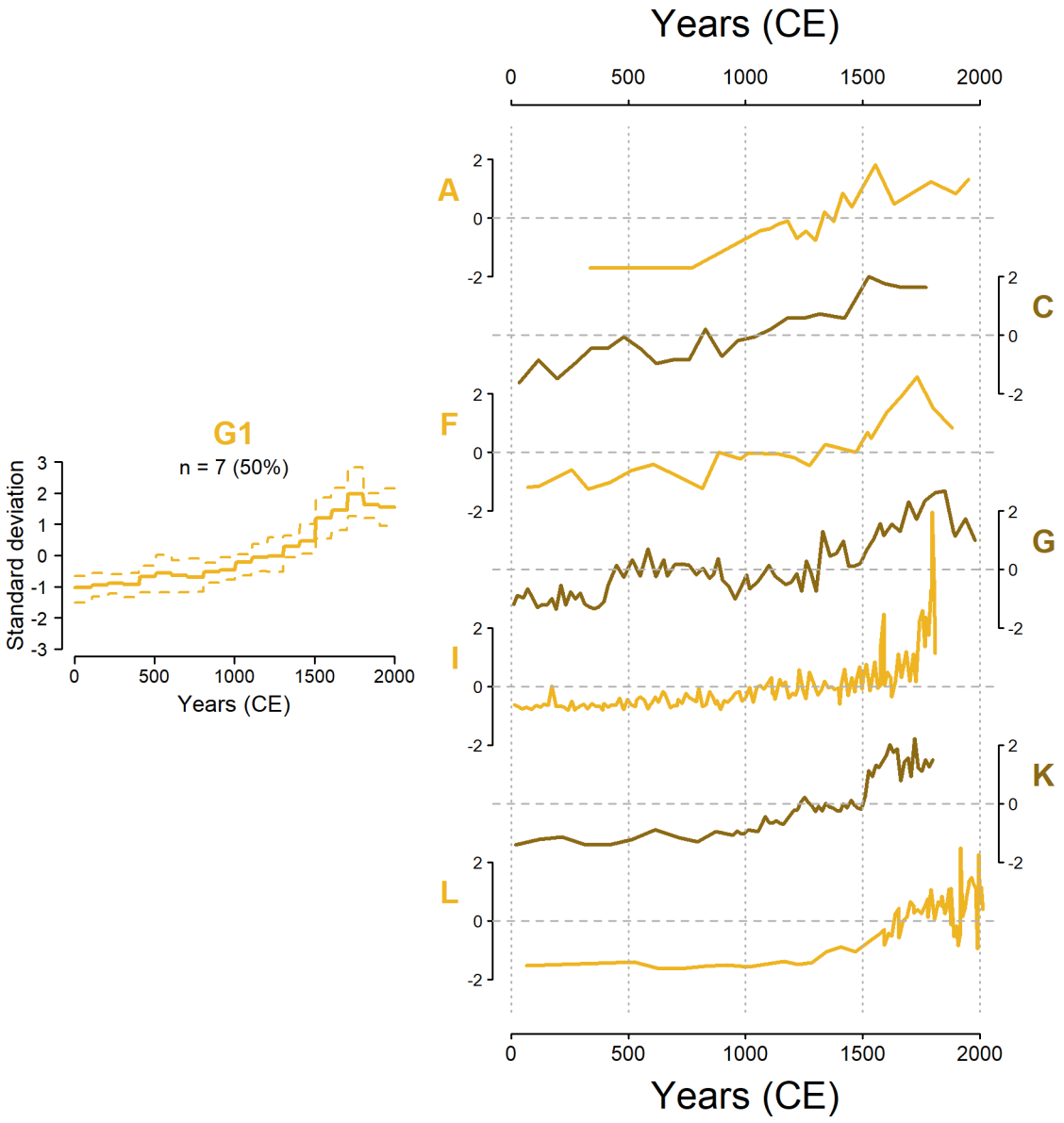

Figure S1. Original data from the records from Group 1 (cluster analysis after removing the global trend).

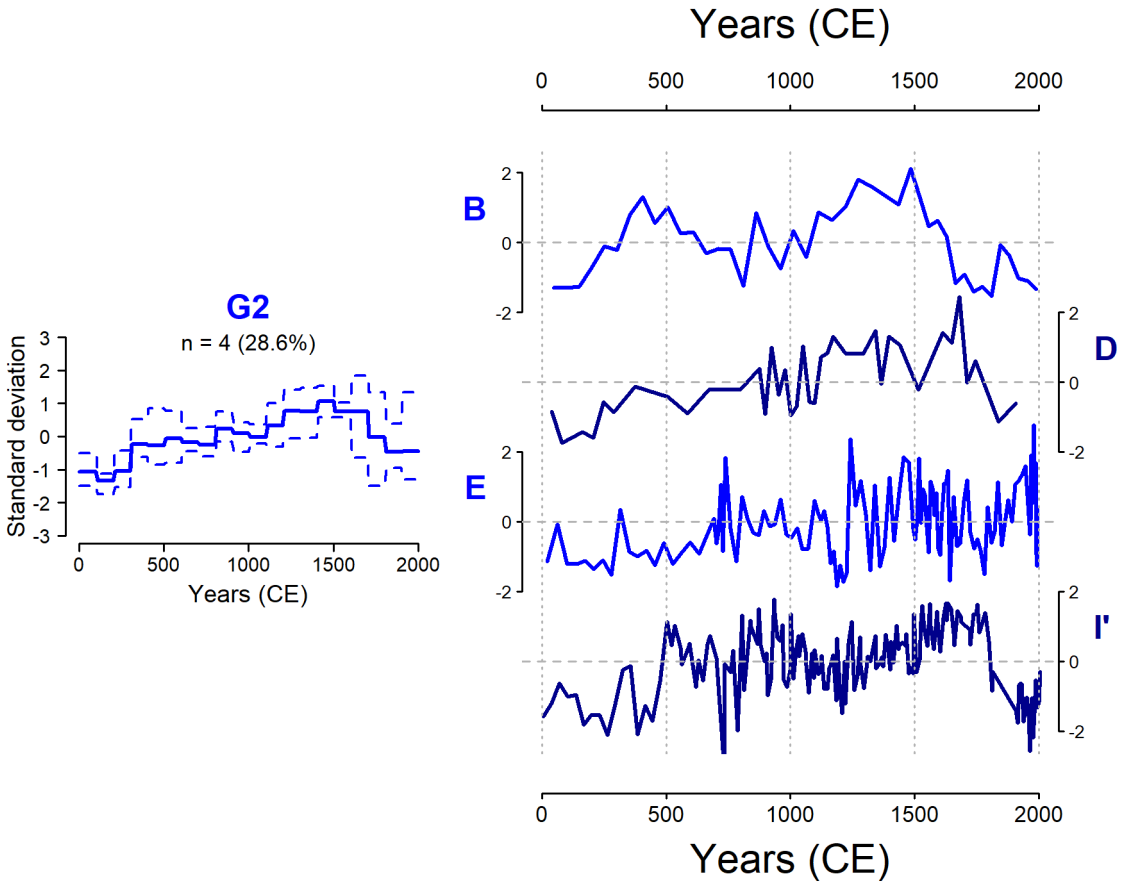

Figure S2. Original data from the records from Group 2 (cluster analysis after removing the global trend).

20

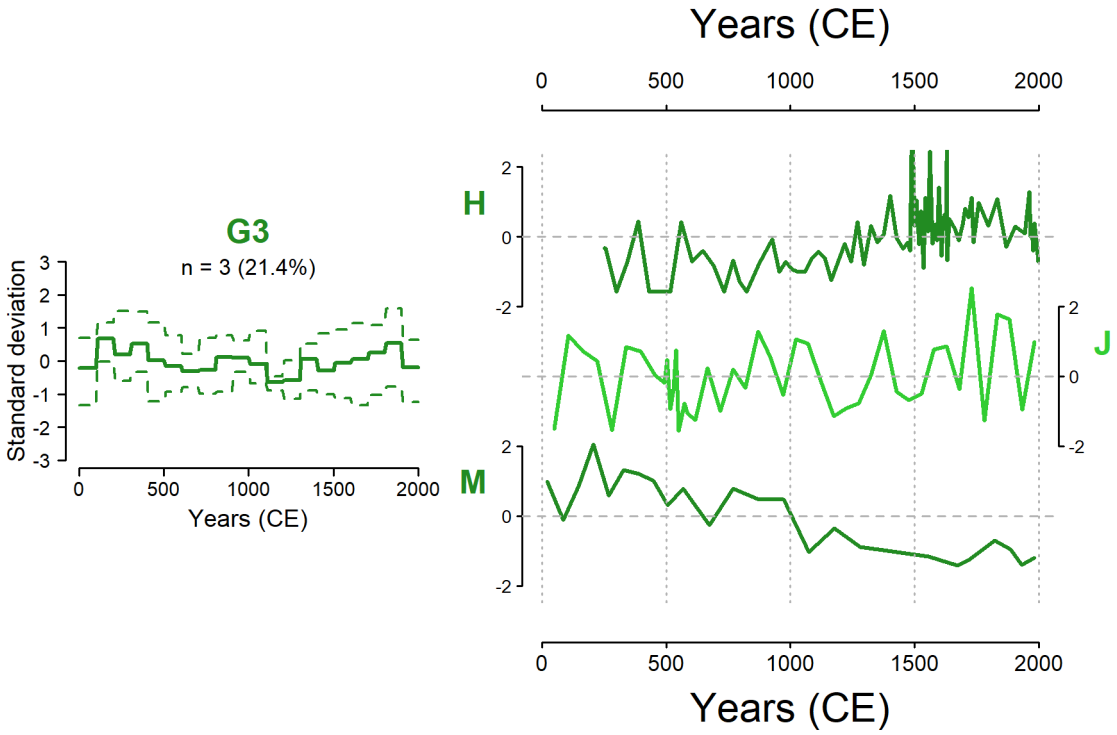

Figure S3. Original data from the records from Group 3 (cluster analysis after removing the global trend).

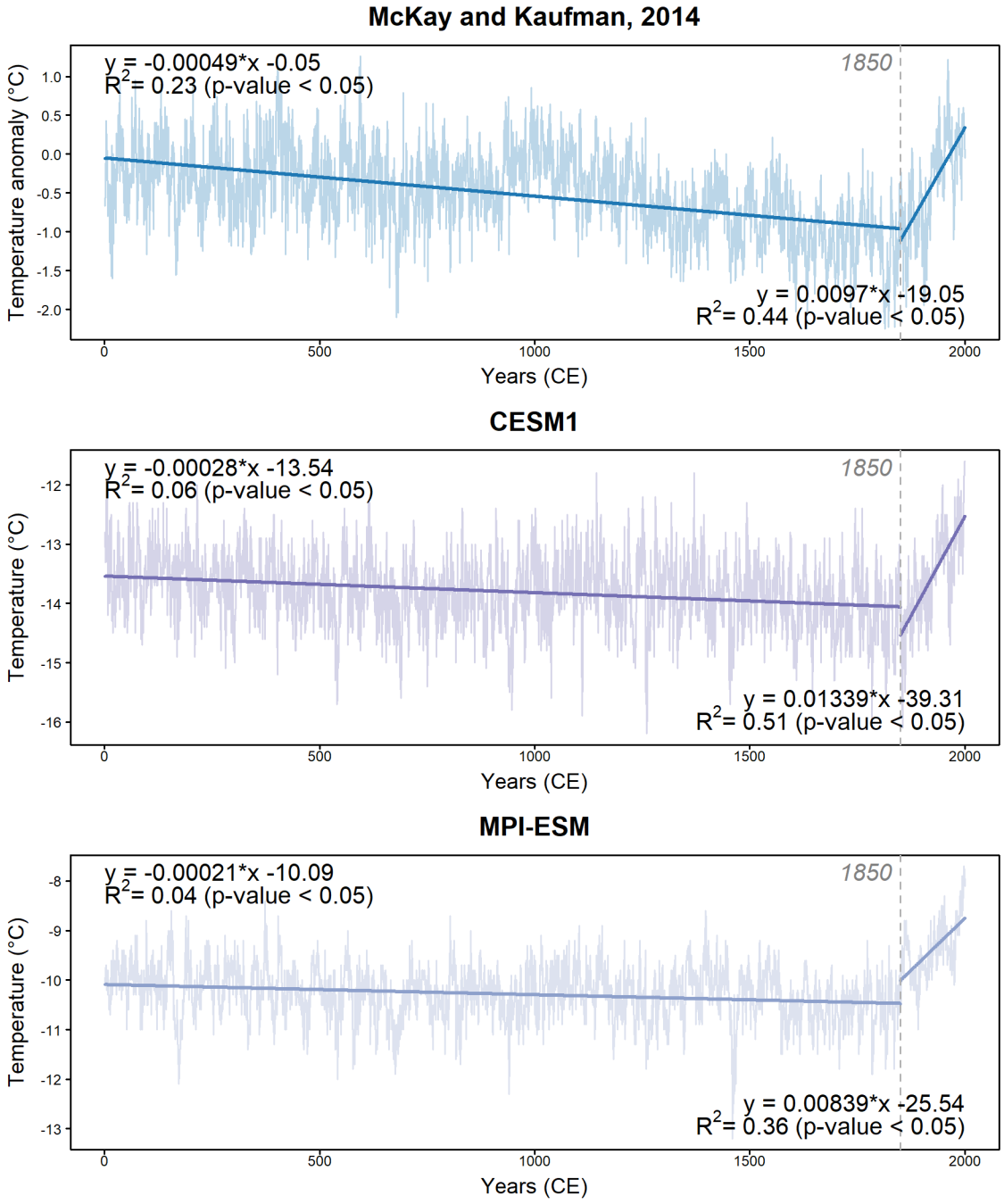

Figure S4. Arctic (latitudes > 60° N) air temperatures based on McKay and Kaufman (2014) and on numerical models CESM1 and MPI-ESM data.

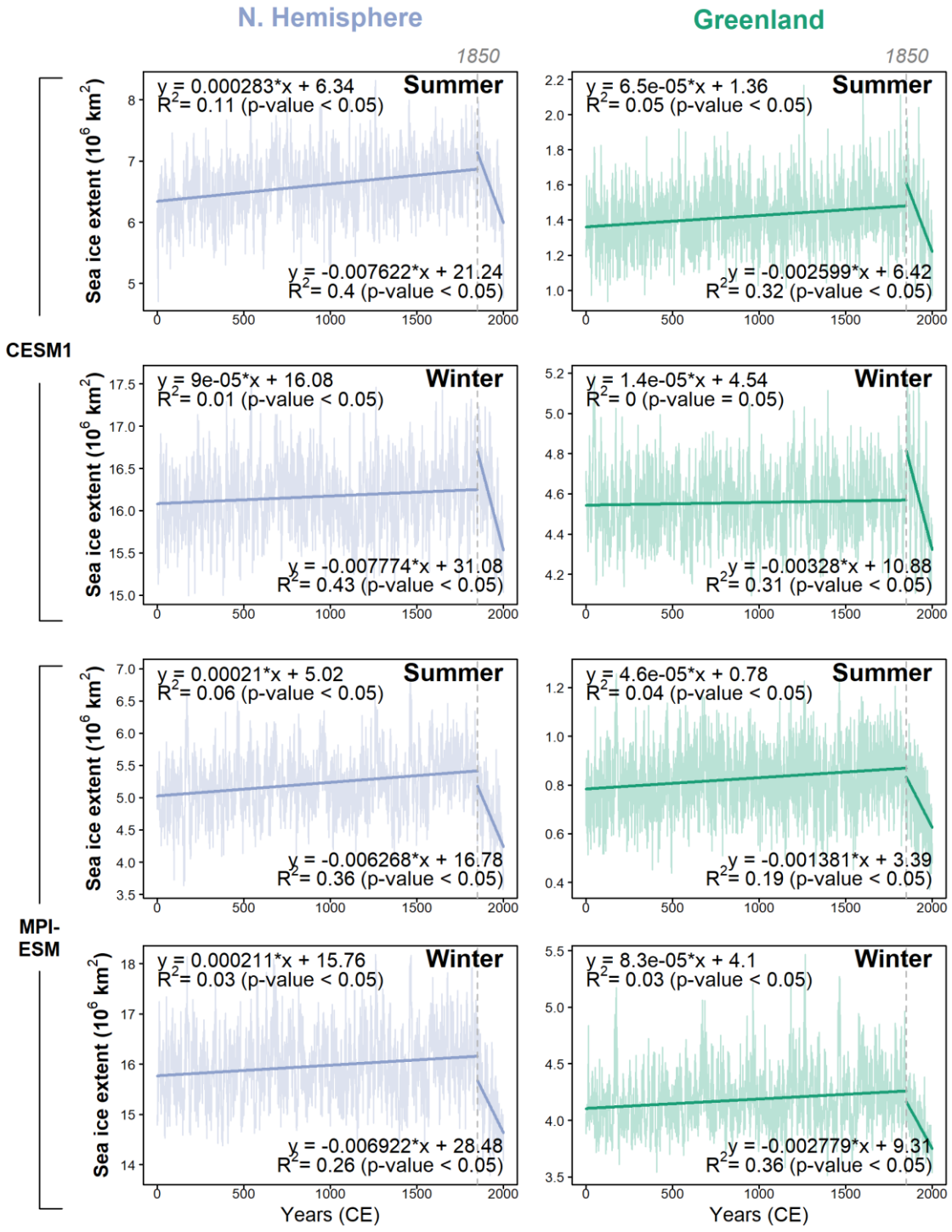

Figure S5. Sea ice extent trends based on numerical models CESM1 and MPI-ESM data, considering the Northern Hemisphere (left column) and region around Greenland (right column), and summer (minimum extent) and winter (maximum extent) seasons.

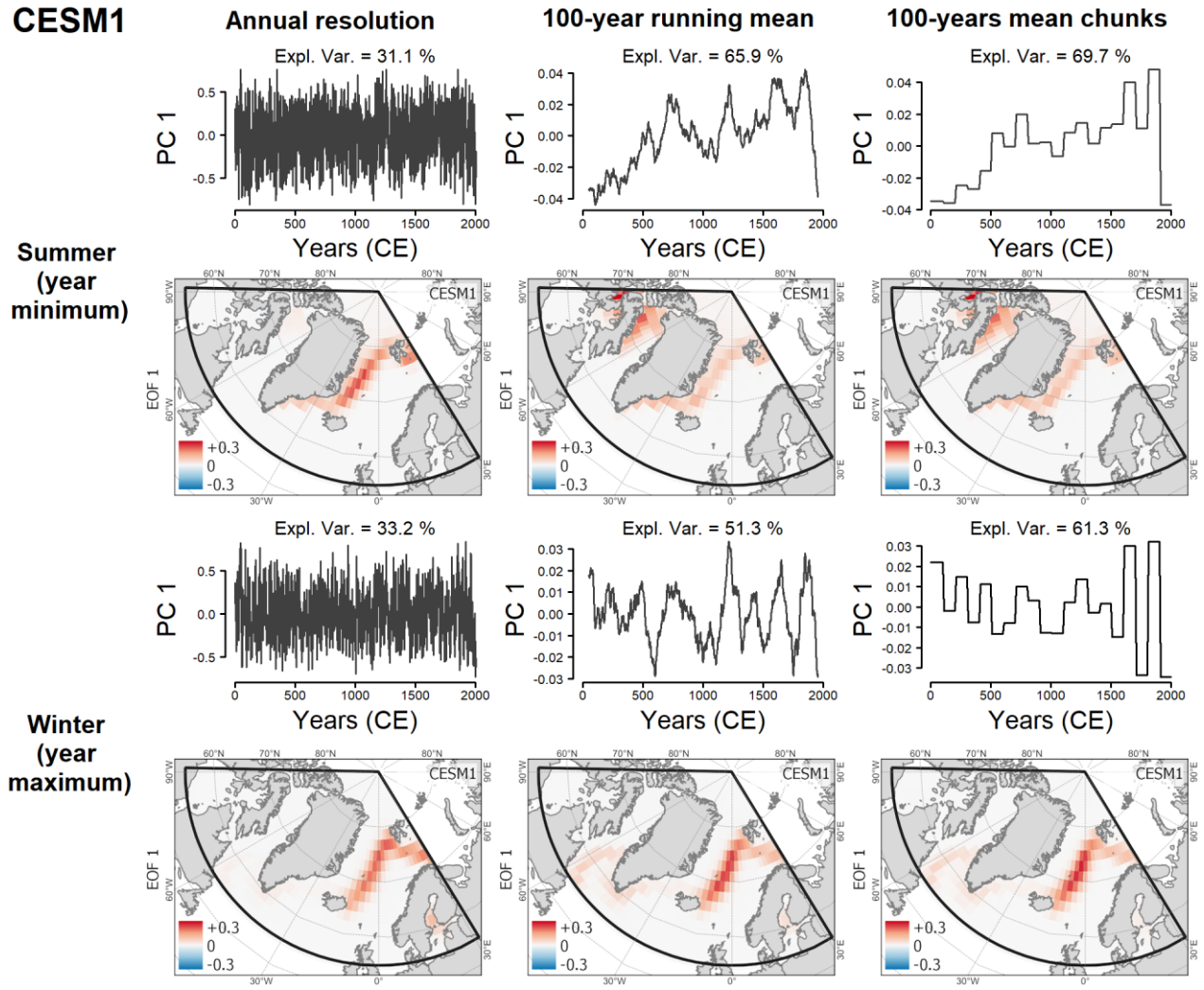

35 **Figure S6. Results of empirical orthogonal function (EOF) analysis (PC1: normalized first principal component; EOF1: first EOF mode loadings) of the sea ice fraction based on CESM1 data, considering summer and winter seasons. First column: Data with annual resolution. Second column: 100-year running mean data. Third column: 100-years mean chunks data.**

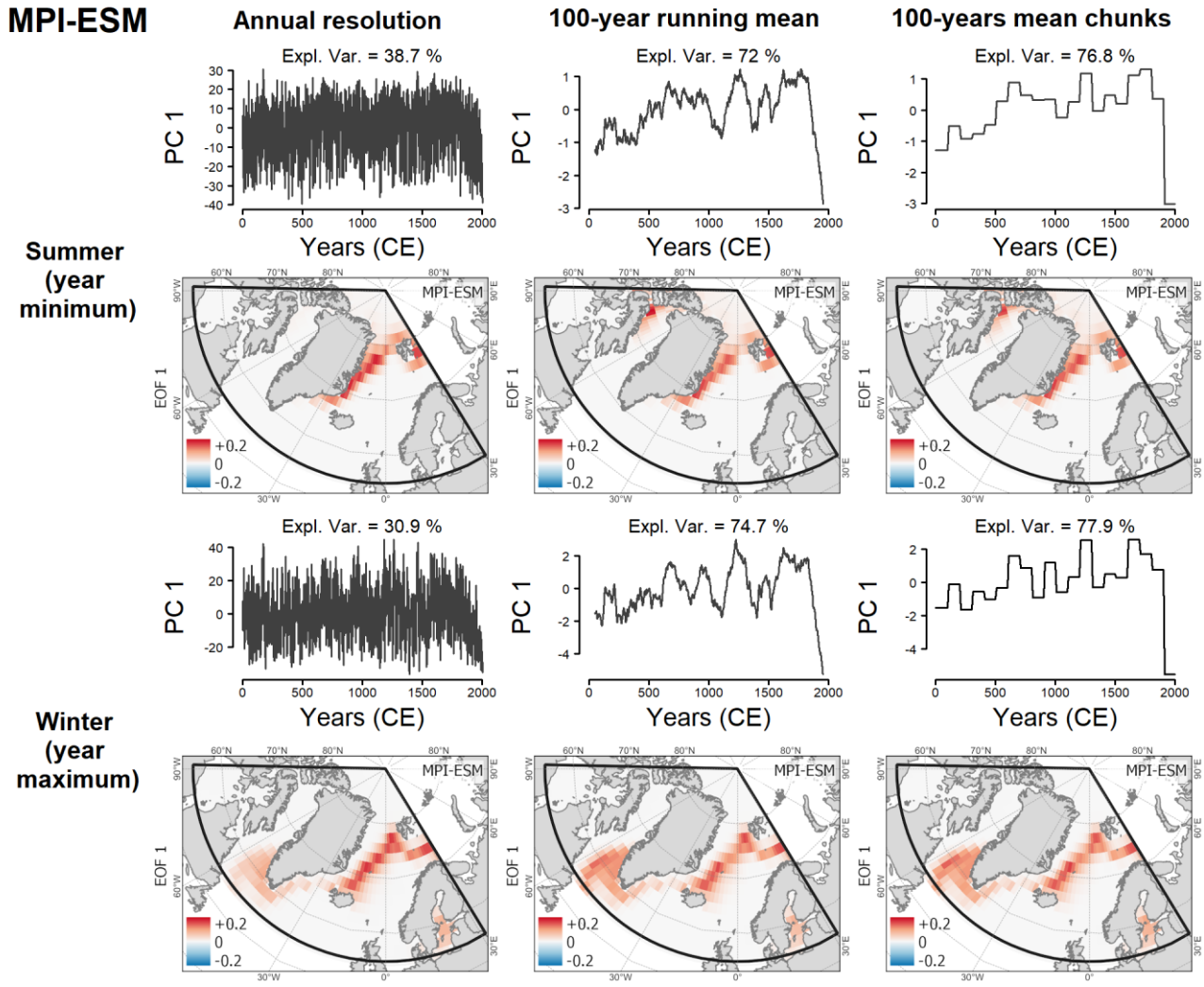

Figure S7. Results of empirical orthogonal function (EOF) analysis (PC1: normalized first principal component; EOF1: first EOF mode loadings) of the sea ice fraction based on MPI-ESM data, considering summer and winter seasons. First column: Data with annual resolution. Second column: 100-year running mean data. Third column: 100-years mean chunks data.

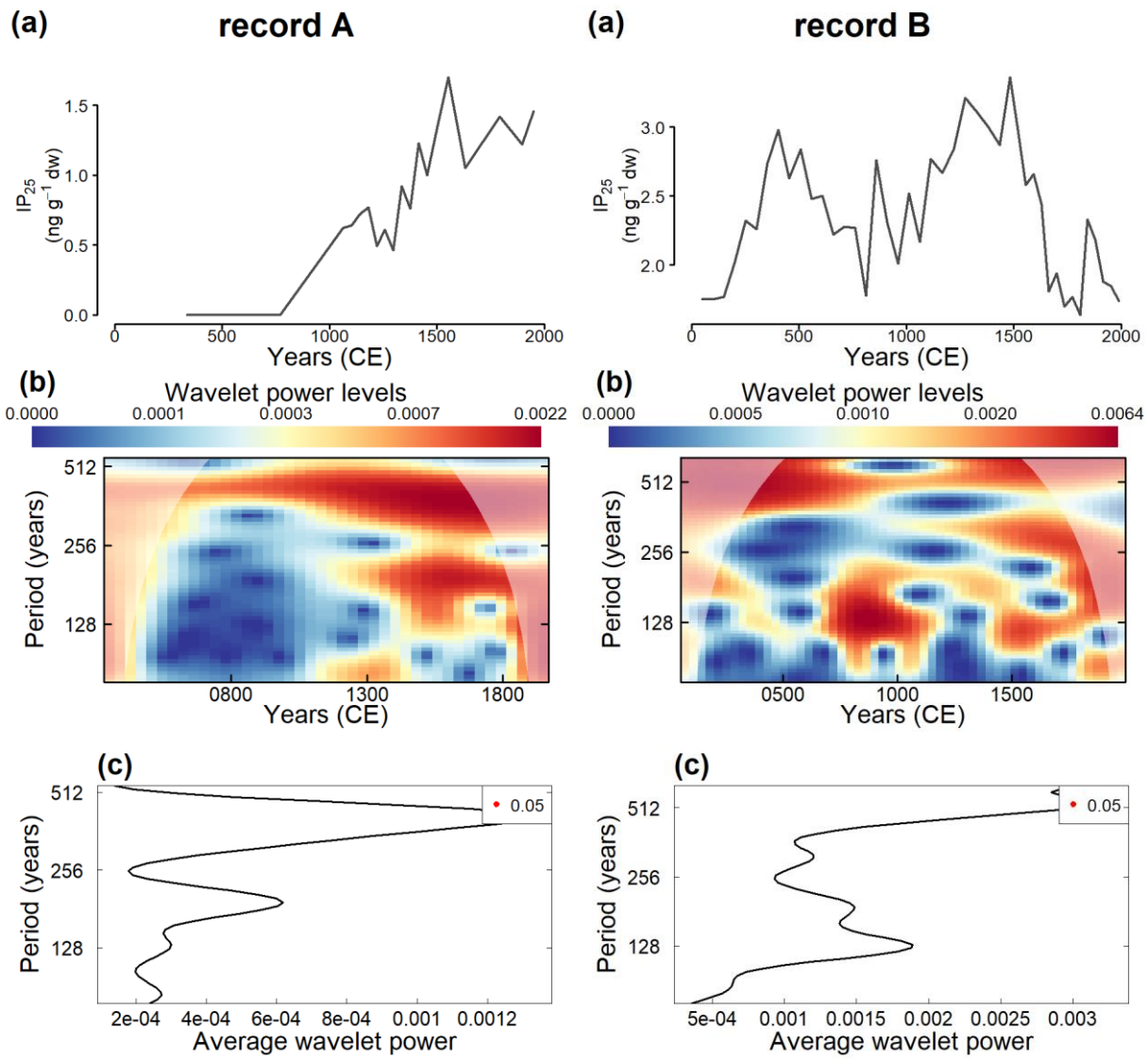

Figure S8. Wavelet analysis of sea ice reconstructions from records A and B. (a) Original time series. (b) Wavelet power spectrum and (c) global wavelet of the normalized signal on the time-frequency domain. Marked regions on the wavelet spectrum indicate significant power to a 95 % confidence interval. The areas under the cone of influence show where edge effects are important.

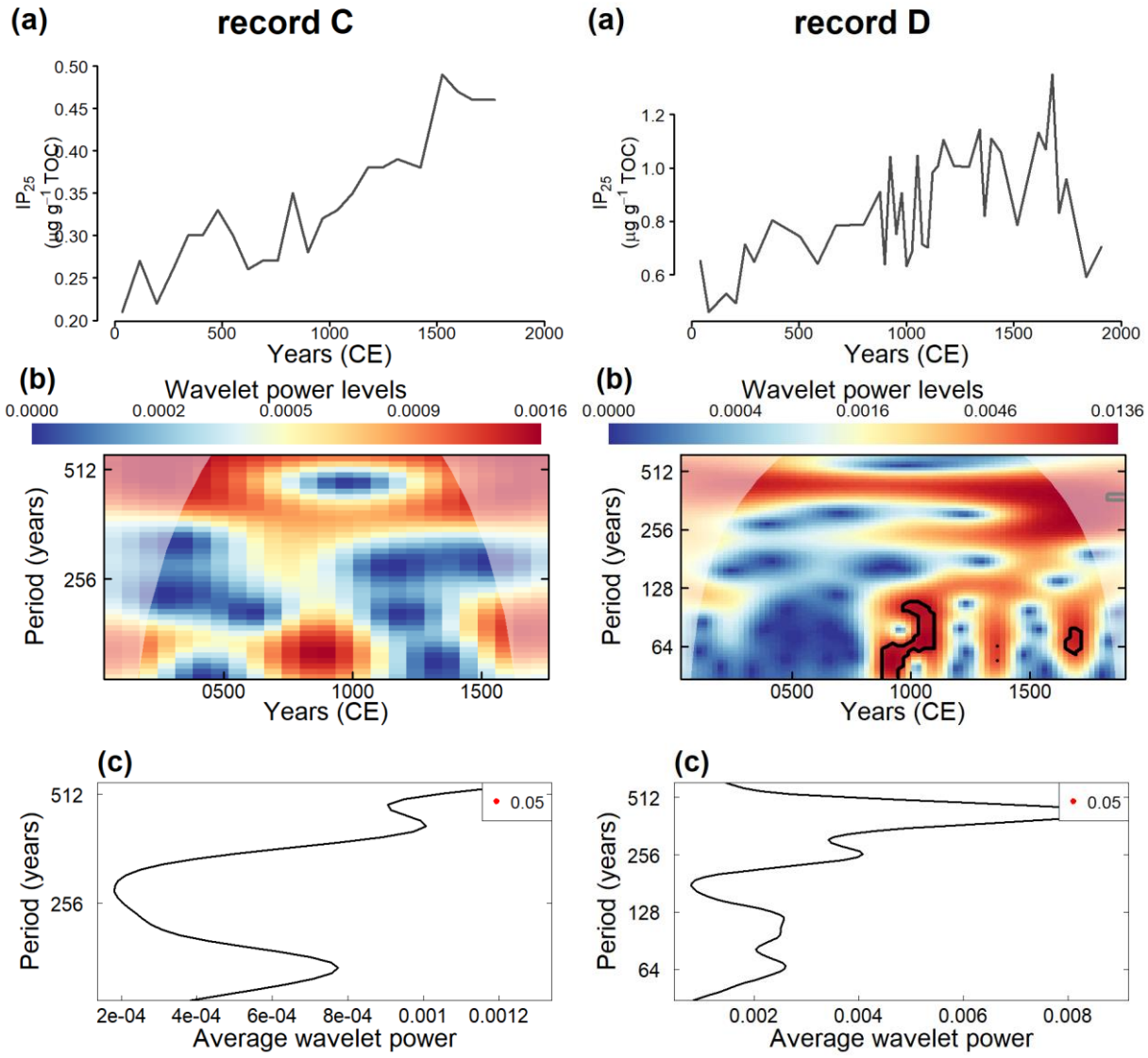

Figure S9. Wavelet analysis of sea ice reconstructions from records C and D. (a) Original time series. (b) Wavelet power spectrum and (c) global wavelet of the normalized signal on the time-frequency domain. Marked regions on the wavelet spectrum indicate significant power to a 95 % confidence interval. The areas under the cone of influence show where edge effects are important.

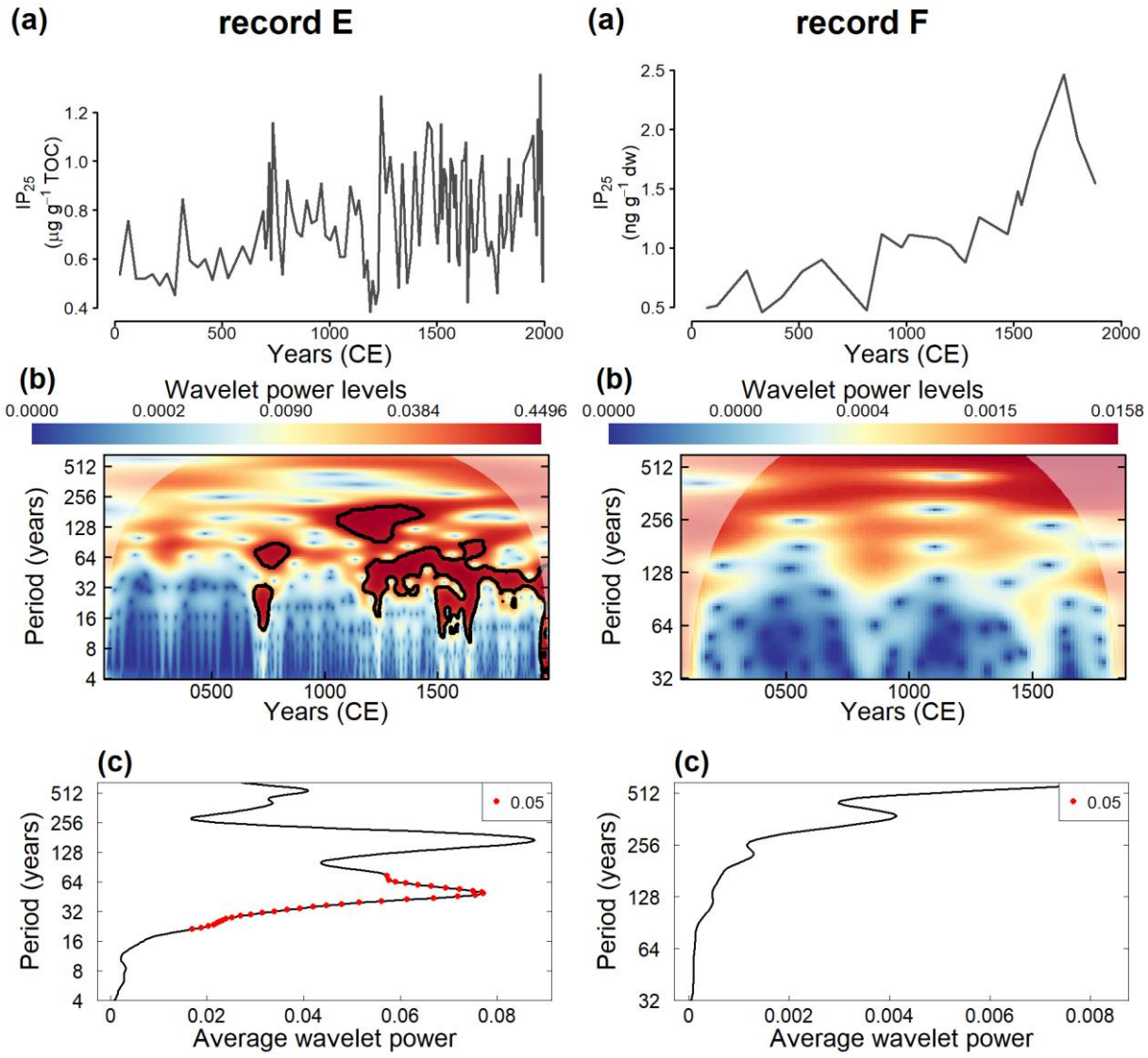

Figure S10. Wavelet analysis of sea ice reconstructions from records E and F. (a) Original time series. (b) Wavelet power spectrum and (c) global wavelet of the normalized signal on the time-frequency domain. Marked regions on the wavelet spectrum indicate significant power to a 95 % confidence interval. The areas under the cone of influence show where edge effects are important.

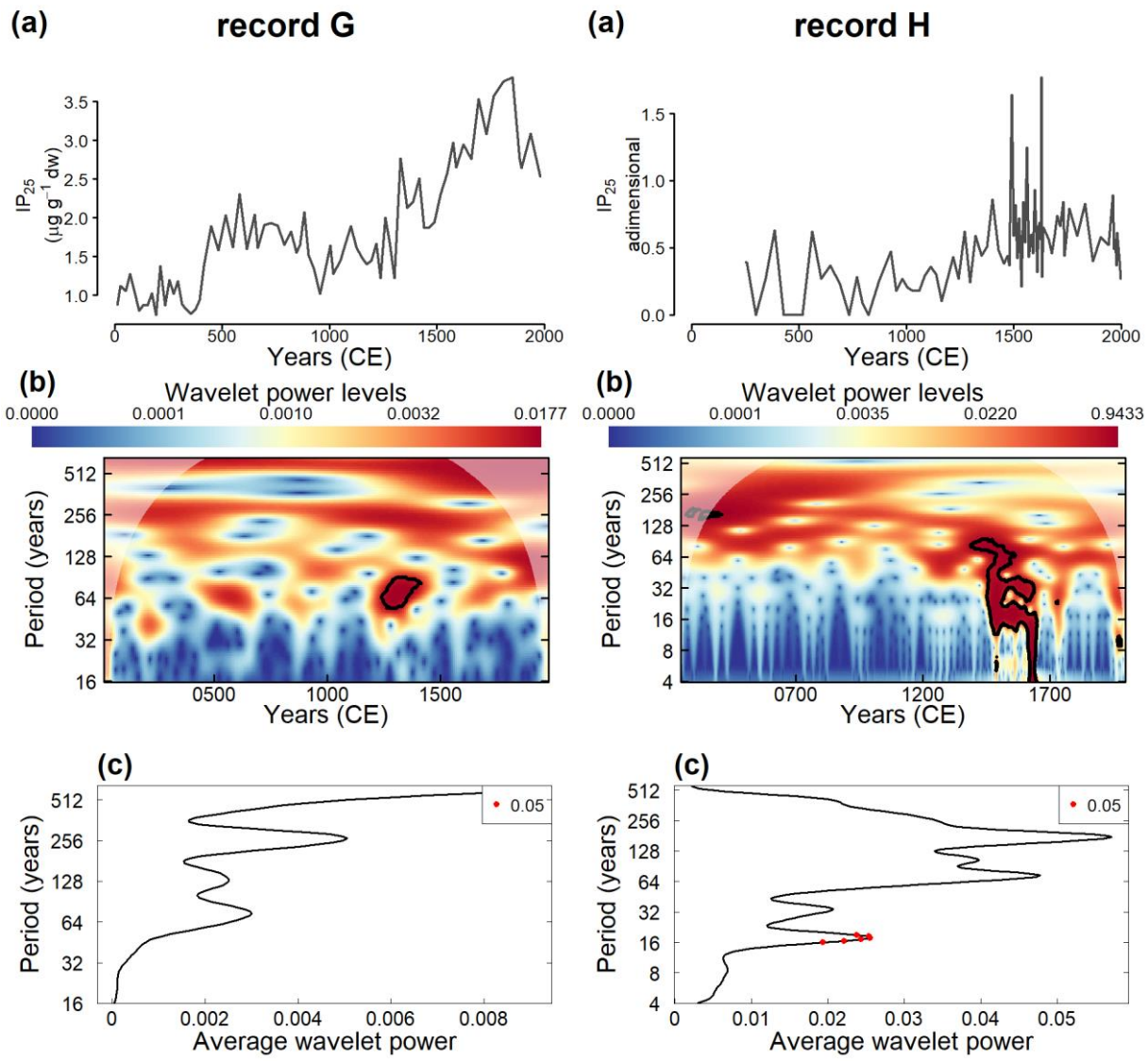

Figure S11. Wavelet analysis of sea ice reconstructions from records G and H. (a) Original time series. (b) Wavelet power spectrum and (c) global wavelet of the normalized signal on the time-frequency domain. Marked regions on the wavelet spectrum indicate significant power to a 95 % confidence interval. The areas under the cone of influence show where edge effects are important.

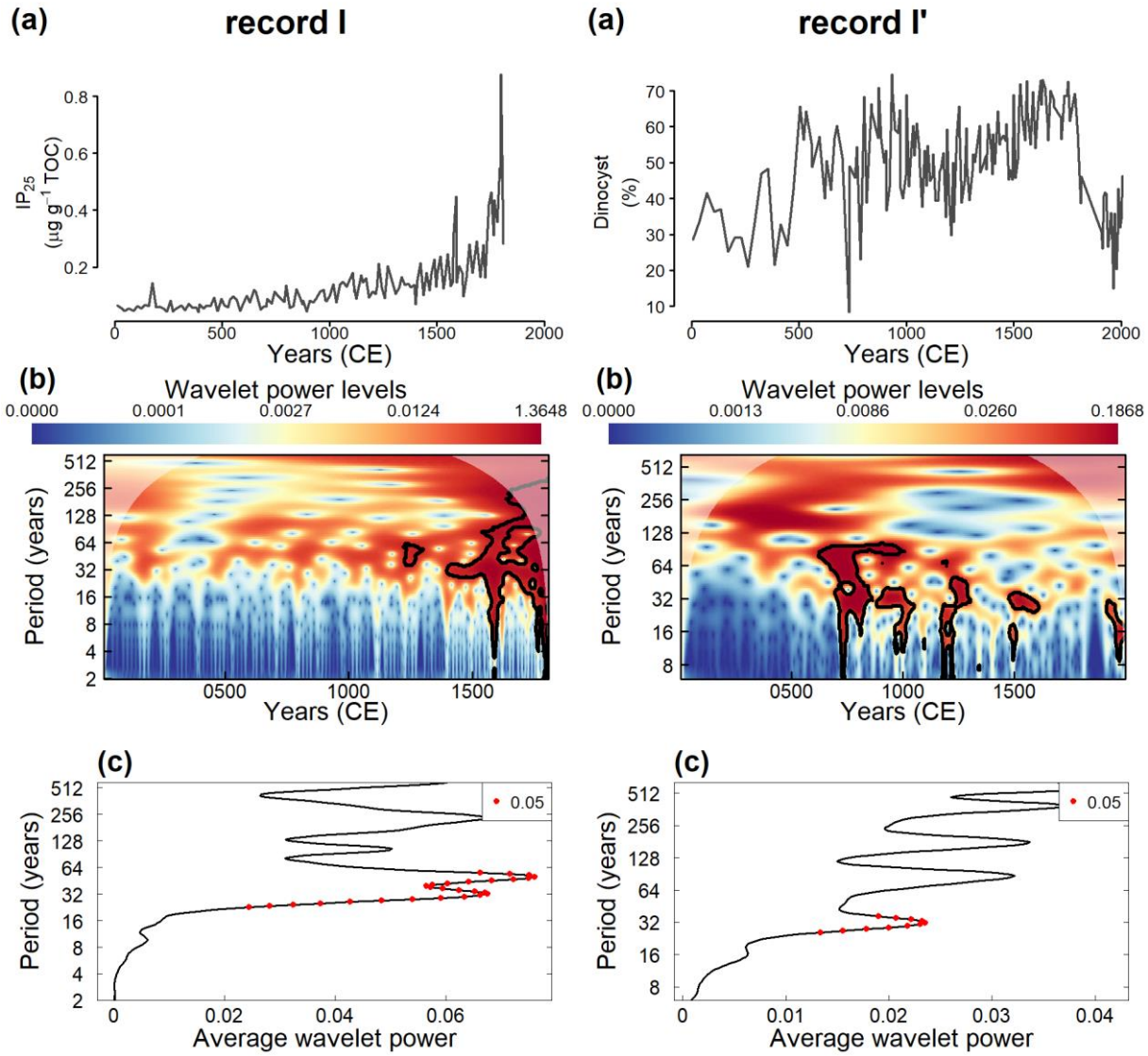

Figure S12. Wavelet analysis of sea ice reconstructions from records I and I'. (a) Original time series. (b) Wavelet power spectrum and (c) global wavelet of the normalized signal on the time-frequency domain. Marked regions on the wavelet spectrum indicate significant power to a 95 % confidence interval. The areas under the cone of influence show where edge effects are important.

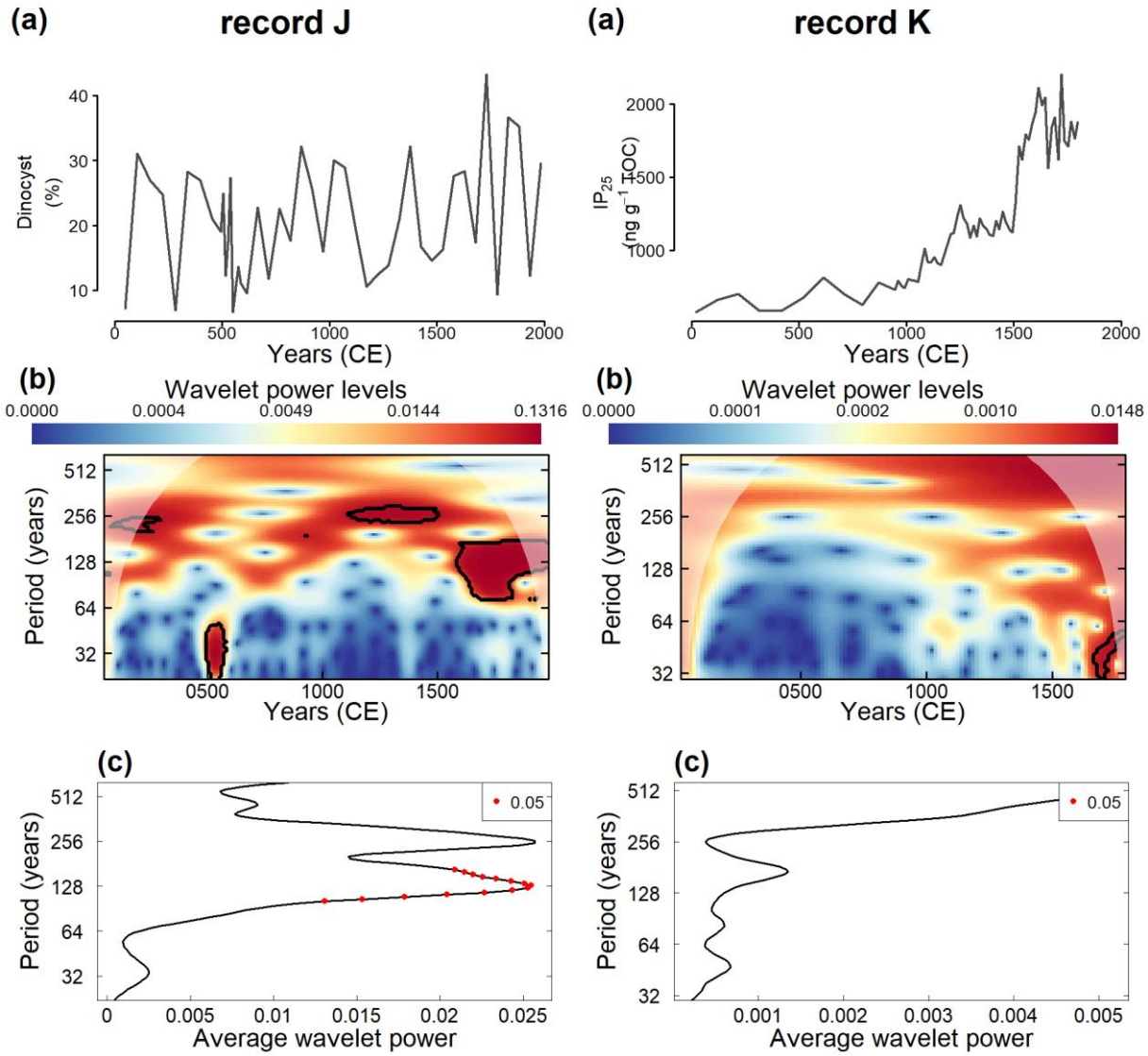

Figure S13. Wavelet analysis of sea ice reconstructions from records J and K. (a) Original time series. (b) Wavelet power spectrum and (c) global wavelet of the normalized signal on the time-frequency domain. Marked regions on the wavelet spectrum indicate significant power to a 95 % confidence interval. The areas under the cone of influence show where edge effects are important.

75

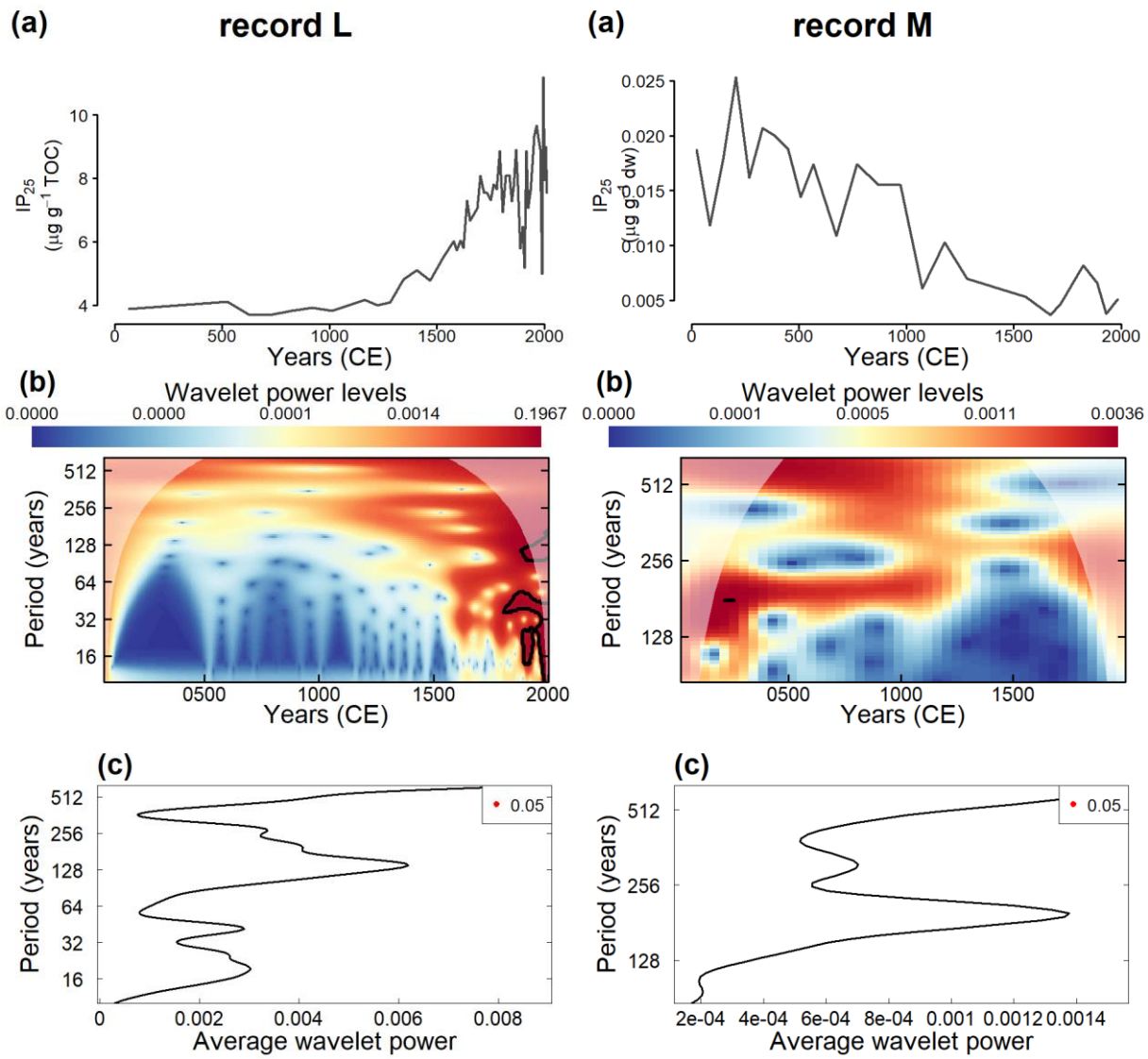

Figure S14. Wavelet analysis of sea ice reconstructions from records L and M. (a) Original time series. (b) Wavelet power spectrum and (c) global wavelet of the normalized signal on the time-frequency domain. Marked regions on the wavelet spectrum indicate significant power to a 95 % confidence interval. The areas under the cone of influence show where edge effects are important.